ASPS Conference Proceedings 1: 1-5 (2022)

Proceedings of

12th Structural Engineering Convention-An International Event (SEC 2022)

Available at https://asps-journals.com/index.php/acp

Buckling Analysis of Laminated Composite Plates under Thermal Conditions

Aman Garg[1,*], H. D. Chalak[2]

[1] Department of Civil Engineering, Research Scholar, National Institute of Technology Kurukshetra, Kurukshetra, 136 119, India
[2] Department of Civil Engineering, Assistant Professor, National Institute of Technology Kurukshetra, Kurukshetra, 136 119, India

Paper ID - 010010

Abstract

In present work, buckling analysis of laminated composite plates is carried out using recently proposed higher-order zigzag theory (HOZT). Third order variation of in-plane displacement field is taken across the thickness of the plate. For predicting the behavior efficiently for thick plates, quadratic variation of transverse displacement field is assumed for core layer and constant for face layers. The present theory satisfies inter-laminar transverse shear stress continuity condition at interface along with zero value at top and bottom surface of the plate. In present study, nine-noded finite element having eleven degrees of freedom per node is used. Present model is free from requirement of any kind of penalty function or C-1 condition.

Keywords: Buckling analysis, laminated plates, finite element, shear stress continuity, HOZT

1. Introduction

Laminated composites are widely used in building various structures because of their property of tailor ability [1]. The demand for high-strength, high-modulus and low-density industrial materials has generated an increased number of applications for fibre laminated composite structures in many different fields such as in submarines, sport equipment, medical instruments, civil engineering, enabling technologies, primary and secondary marine and aerospace structures, astronavigation and many more industries [2]. However, all these structures are expected to serve under changing environmental conditions (such as under different temperature or moisture). The stresses arising due to change in temperature are called as thermal stresses. If these stresses are not included during analysis/design stage, it may result in failure of structure.

The analysis of laminated composite plates under thermal conditions is carried out by several researchers using different theories and methods. The simplest theory available is called as classical laminated theory (CLT). However, this theory neglects transverse deformations and hence is not able to predict true behavior of composites. This problem is solved by shear deformation theories. The simplest shear deformation theory is known as first-order shear deformation theory (FOSDT). This theory assumes constant transverse deformation. Some of the works regarding use of FODST for thermally induced buckling analysis of laminated composite plates are [3,4]. The main problem with this theory is incorporation of shear correction factor.The value of the shear correction factor depends upon a number of factors such as end conditions, geometrical properties, etc. [5].

However, the problem of inclusion of shear correction factor has been solved by using higher-order shear deformation theories (HOSDTs). Singh et al. [6] highlighted the benefits of inclusion of higher order terms during buckling analysis of laminated composite plates. Works available in literature regarding use of HOSDT for analysis laminated composite plates are [7-11]. A number of HOSDTs are available in the literature which differs from each other in the form of distribution of transverse shear stresses across the thickness. Highlighting the problems associated with HOSDT, Chakrabarti et al. [12] stated, “These theories predicted the continuous transverse shear strain across the thickness at interfaces with a discontinuity in the transverse shear stresses at interfaces. But the actual behavior of LCs is entirely different that is, the transverse shear stresses at interfaces must be continuous although discontinuity in transverse shear strains may exist. Also, additional dependent unknowns are introduced in HSDT with each new adding power of thickness coordinate. Even these theories do not satisfy the stress-free condition at the top and the bottom face of the laminated structure.”

To handle the problem posed by HOSDTs, layerwise theories (LWT) are developed. In these theories, each layer is analyzed separately and the results are integrated over the entire thickness of the structure. Works available in literature on the application of LWTs for thermally induced buckling analysis are [13,14]. Regarding the application of LWTs, Chalak et al. [15] stated, “The main issue with these type of

*Corresponding author. Tel: +918813971517; E-mail address: amang321@gmail.com

Published online: December 19, 2022
doi:10.38208/acp.v1.463

theories lies in the handling of the number of unknowns. With the increase in the number of layers, the unknown increases which are difficult to evaluate. Thus, these theories are computationally inefficient for multi-layered structures." Another class of LWTs called as refined layerwise theory or zigzag theory.

In zigzag theories, the unknowns at each layer are defined with respect to unknowns at reference layer. This class of theory satisfies inter-laminar transverse shear stress continuity condition at interface along with zero value at top and bottom of plate. works available in literature pertaining used of higher-order zigzag theory (HOZT) for analysis of laminated composite plates under thermal conditions are [16-20]. Noor and Burton [21,22] presented 3D solutions for studying buckling behavior of laminated composite plates under thermal conditions. Recently, Garg and Chalak [23] presented a detailed review on the analysis of laminated composite and sandwich plates under hygrothermal conditions.

In present work, buckling analysis of laminated composite plates is carried out by using recently proposed HOZT which includes transverse displacement field [24,25].

2. Mathematical Modelling

The formulation is based on the following assumptions:

- The middle plane of the plate is taken as reference plane.
- The laminated plates consist of a number of layers bonded together.
- The layers are perfectly bonded with each other.
- The orthotropic layers may have any orientation with respect to the reference structural (plate) axes system.
- The materials used obey Hooke's law.
- The in-plane displacement is taken asthird-order variation across the plate thickness with kinks at the layer interfaces according to HOZT.
- Cubic variation of displacement field along x- and y-axis can be stated as (Fig. 1):

$$U^{(x)} = u^{(0)} + z\psi^{(x)} + \sum_{i=1}^{n^{(u)}-1}\left(z - z_i^{(u)}\right)H\left(z - z_i^{(u)}\right)E_i^{(xu)} + \sum_{j=1}^{n^{(l)}-1}\left(z - z_j^{(u)}\right)H\left(-z + z_j^{(u)}\right)E_j^{(xl)} + \zeta^{(x)}z^2 + \mu^{(x)}z^3 \quad (1)$$

$$V^{(y)} = v^{(0)} + z\psi^{(y)} + \sum_{i=1}^{n^{(u)}-1}\left(z - z_i^{(l)}\right)H\left(z - z_i^{(l)}\right)E_i^{(yu)} + \sum_{j=1}^{n^{(l)}-1}\left(z - z_j^{(l)}\right)H\left(-z + z_j^{(l)}\right)E_j^{(yl)} + \zeta^{(y)}z^2 + \mu^{(y)}z^3 \quad (2)$$

Quadratic variation of transverse displacement is taken quadratic for core layer while it is taken constant for face layer (Fig. 2):

$$W^{(z)} = l^{(1)}w^{(u)} + l^{(2)}w^{(0)} + l^{(3)}w^{(l)}(forcore) = w^{(u)}(forupperfacelayer) = w^{(u)}(forlowerfacelayer) \quad (3)$$

For an orthotropic lamina, the stress-strain relationship can be written as:

$$\{\bar{\sigma}\}_{(6\times1)} = [\overline{Q_k}]_{(6\times6)}[\{\bar{\varepsilon}\}_{(6\times1)} - \{\alpha\}\Delta T - \{\beta\}\Delta C] \quad \text{or} \quad \{\bar{\sigma}\} = [\overline{Q_k}]\{\bar{\varepsilon}\}_{net} \quad (4)$$

where, $\{\bar{\varepsilon}\}_{net} = \{\bar{\varepsilon}\} - \{\bar{\varepsilon}\}_{thermal}$

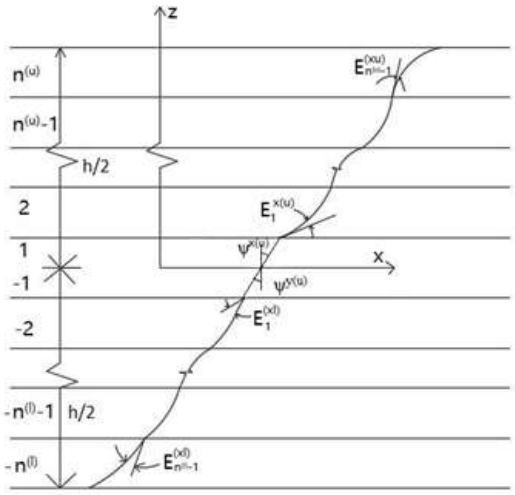

Fig. 1. In-plane displacement variation for laminated composite plate.

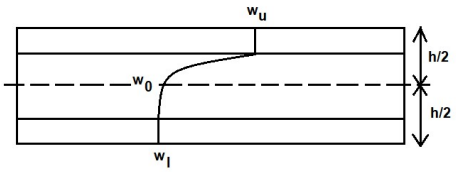

Fig. 2. Transverse displacement variation across thickness of laminated composite plate.

Imposing shear stress continuity condition in transverse direction at layer interface, zero or transverse shear stress free condition at top and bottom of plate and conditions of $U = u^{(u)}, V = v^{(u)}$ at top of the plate and $U = u^{(l)}, V = v^{(l)}$at bottom of the plate,

$\zeta^{(x)}, \zeta^{(y)}, \mu^{(x)}, \mu^{(y)}, E_i^{(xu)}, E_j^{(xl)}, E_i^{(yu)}, E_j^{(yl)}, (\partial w_u/\partial x), (\partial w_l/\partial x), (\partial w_u/\partial y), (\partial w_l/\partial y)$ can be written in form of displacements $u^{(0)}, v^{(0)}, \psi^{(x)}, \psi^{(y)}, u^{(u)}, u^{(l)}, v^{(u)}, v^{(l)}$as:

$$[B] = \begin{matrix}[\zeta^{(x)}\eta^{(x)}\zeta^{(y)}\eta^{(y)}E_1^{(xu)}E_2^{(xu)} \dots E_{n^{(u)}-1}^{(xu)}E_1^{(xl)}E_2^{(xl)} \\ \dots E_{n^{(l)}-1}^{(xl)}E_1^{(yu)}E_2^{(yu)} \dots E_{n^{(u)}-1}^{(yu)}E_1^{(yl)}E_2^{(yl)} \dots E_{n^{(l)}-1}^{(yl)} \\ \left(\partial w^{(u)}/\partial x\right)\left(\partial w^{(l)}/\partial x\right)\left(\partial w^{(u)}/\partial y\right)\left(\partial w^{(l)}/\partial y\right)]^T\end{matrix}$$

$$\left\{u^{(0)}, v^{(0)}, \psi^{(x)}, \psi^{(y)}, u^{(u)}, u^{(l)}, v^{(u)}, v^{(l)}\right\}^T$$

or $[B] = [A]\{F\}$ (5)

Elements of [A] are function of material properties. Since last four entries in [B] represents derivative of transverse displacement field at top and bottom of plate in terms of elements of {F} helps in eliminating problem associated with C-1 continuity requirements.

Using elements of {F}, Eq. (1) & (2) can be written as:

$$U = b^{(1)}u^{(0)} + b^{(2)}v^{(0)} + b^{(3)}\psi^{(x)} + b^{(4)}\psi^{(y)} + b^{(5)}u^{(u)} + b^{(6)}v^{(u)} + b^{(7)}u^{(l)} + b^{(8)}v^{(l)} \quad (6)$$

$$V = c^{(1)}u^{(0)} + c^{(2)}v^{(0)} + c^{(3)}\psi^{(x)} + c^{(4)}\psi^{(y)} + c^{(5)}u^{(u)} + c^{(6)}v^{(u)} + c^{(7)}u^{(l)} + c^{(8)}v^{(l)} \quad (7)$$

Coefficients b^i's and c^i's are function of thickness coordinates, material properties and unit step function.

Applying four additional conditions of satisfying displacement along x- and y- directions at top and bottom of plate, derivatives of transverse displacements can be written in form of nodal field variables appearing in Eq. (5). Hence, Eq. (6) & (7) is free from any kind of C-1 continuity

requirements without defining new field variables or incorporating any kind of penalty function.

Using Eq. (3), (6) & (7) the generalised displacement vector $\{\gamma\}$ can be written as:

$$\{\gamma\} = \left\{u^{(0)} v^{(0)} w^{(0)} \psi^{(x)} \psi^{(y)} u^{(u)} v^{(u)} w^{(u)} u^{(l)} v^{(l)} w^{(l)}\right\}^T$$

With the help of unknowns, linear train-displacement relationships can be written as:

$$\{\bar{\varepsilon}\}_{(6\times1)} = \left[\frac{\partial U}{\partial x}\frac{\partial V}{\partial y}\frac{\partial W}{\partial z}\frac{\partial U}{\partial x} + \frac{\partial V}{\partial y}\frac{\partial U}{\partial z} + \frac{\partial W}{\partial x}\frac{\partial V}{\partial z} + \frac{\partial W}{\partial x}\right] or = [H]_{(6\times33)}\{\varepsilon\}_{(33\times1)} \quad (8)$$

where elements of [H] are function of unit step function and z

Using nine-noded quadratic finite element having eleven degrees of freedom per node $\{u^{(0)}, v^{(0)}, w^{(0)}, \psi^{(x)}, \psi^{(y)}, u^{(u)}, v^{(u)}, w^{(u)}, u^{(l)}, v^{(l)}, w^{(l)}\}$, generalised displacement vector can be written as:

$$\gamma = \sum_{i=1}^{11} N_i \gamma_i \quad (9)$$

Using above Eq., Eq. (8) can be written in term of unknowns as:

$$\{\varepsilon\}_{(6\times1)} = [B]_{(6\times99)}\{\gamma\}_{(99\times1)} \quad (10)$$

where [B] is strain-displacement relationship in Cartesian coordinate system.

Writing strain-displacement relationship in linear range, and with the help of Equations (1) - (6), the strains can be written in form of unknowns as:

$$\{\bar{\varepsilon}\} = \{\bar{\varepsilon}\}_{Linear} + \{\bar{\varepsilon}\}_{Non-linear} \quad (11)$$

where,

$\{\bar{\varepsilon}\}_{Linear}$ can be calculated as per Equation (8).

$\{\bar{\varepsilon}\}_{Linear} = [H]\{\varepsilon\}_{Linear}$,

$$\{\bar{\varepsilon}\}_{Non-linear} = \begin{bmatrix} \frac{1}{2}\left(\frac{\partial U_{(z)}}{\partial x}\right)^2 + \frac{1}{2}\left(\frac{\partial U_{(x)}}{\partial x}\right)^2 + \frac{1}{2}\left(\frac{\partial U_{(y)}}{\partial x}\right)^2 \\ \frac{1}{2}\left(\frac{\partial U_{(z)}}{\partial y}\right)^2 + \frac{1}{2}\left(\frac{\partial U_{(x)}}{\partial y}\right)^2 + \frac{1}{2}\left(\frac{\partial U_{(y)}}{\partial y}\right)^2 \\ \left(\frac{\partial U_{(z)}}{\partial x}\right)\left(\frac{\partial U_{(z)}}{\partial y}\right) + \left(\frac{\partial U_{(x)}}{\partial x}\right)\left(\frac{\partial U_{(x)}}{\partial y}\right) + \left(\frac{\partial U_{(y)}}{\partial x}\right)\left(\frac{\partial U_{(y)}}{\partial y}\right) \end{bmatrix}$$

$$\{\bar{\varepsilon}\}_{Non-linear} = \frac{1}{2}\begin{bmatrix} \frac{\partial U_{(z)}}{\partial x} & 0 & \frac{\partial U_{(x)}}{\partial x} & 0 & \frac{\partial U_{(y)}}{\partial x} & 0 \\ 0 & \frac{\partial U_{(z)}}{\partial y} & 0 & \frac{\partial U_{(x)}}{\partial y} & 0 & \frac{\partial U_{(y)}}{\partial y} \\ \frac{\partial U_{(z)}}{\partial y} & \frac{\partial U_{(z)}}{\partial x} & \frac{\partial U_{(x)}}{\partial y} & \frac{\partial U_{(x)}}{\partial x} & \frac{\partial U_{(y)}}{\partial y} & \frac{\partial U_{(y)}}{\partial x} \end{bmatrix} \times \begin{Bmatrix} \frac{\partial U_{(z)}}{\partial x} \\ \frac{\partial U_{(z)}}{\partial y} \\ \frac{\partial U_{(x)}}{\partial x} \\ \frac{\partial U_{(x)}}{\partial y} \\ \frac{\partial U_{(y)}}{\partial x} \\ \frac{\partial U_{(y)}}{\partial y} \end{Bmatrix} = \frac{1}{2}[A_G][\Lambda] = \frac{1}{2}[H_G][B]\{\delta\}$$

and the elements contained in $[H], [A_G]$ and $[H_G]$ are function of unit step function and thickness coordinate and $[B]$ is the strain-displacement relationship in Cartesian coordinates.

With the matrix $[B]$ in the above equation, the geometric stiffness matrix $[K_{ge}]$ can be derived and may be written as

$$[K_{ge}] = \sum_{i=1}^{nu+nl} \iiint [B]^T [S^k][B] dxdydz \quad (12)$$

where $[S^k]$ is the in-plane stress components of the kth layer can be written as

$$[S^k] = \begin{bmatrix} \sigma_{xx} & \tau_{xy} & 0 & 0 & 0 & 0 \\ \tau_{xy} & \sigma_{yy} & 0 & 0 & 0 & 0 \\ 0 & 0 & \sigma_{xx} & \tau_{xy} & 0 & 0 \\ 0 & 0 & \tau_{xy} & \sigma_{yy} & 0 & 0 \\ 0 & 0 & 0 & 0 & \sigma_{xx} & \tau_{xy} \\ 0 & 0 & 0 & 0 & \tau_{xy} & \sigma_{yy} \end{bmatrix}$$

The total potential energy of the plate under hygrothermal and transverse load may can be written as:

$$\Pi_e = U_s - W_{ext} \quad (13)$$

where, U_S is the plate's strain energy and W_{ext} is the energy due to external loading.

$$U_s = \frac{1}{2}\sum_{k=1}^{n} \iiint \{\bar{\varepsilon}_{net}\}^T [\bar{C}]_k \{\bar{\varepsilon}_{net}\} dxdydz \quad (14)$$

$$U_{s=} \frac{1}{2}\iint [\{\varepsilon\}^T [D]\{\varepsilon\}] dxdy - \iint \{\varepsilon\}^T [f^{hygrothermal}] dxdy + \frac{1}{2}\sum_{k=1}^{n} \iiint \{\varepsilon_{hygrothermal}\}^T [\bar{Q}]_k \{\varepsilon_{hygrothermal}\} dxdydz \quad (15)$$

where,

$$[D] = \sum_{k=1}^{n} \int [H]^T [\bar{Q}]_k [H] dz \quad \text{and} \quad [f^{hermal}] = \sum_{k=1}^{n} \int [H]^T [\bar{Q}]_k [\varepsilon_{therm}\ ] dz$$

While applying the principle of minimum potential energy, the last term appearing in the Equation (2.15) will vanish. The energy due to external load = 0 because no external mechanical load is acting on the plate. Only thermal loading is acting on the plate.

Now, calculating the elemental potential energy by combining Equations (2.12), (2.14) as

$$\Pi_e = (1/2) \iint \{\delta\}^T [B]^T [D][B]\{\delta\} dxdy - (1/2) \iint \{\delta\}^T [B]^T [f^{hygrothermal}] dxdy$$

$$\Pi_e = (1/2)\{\delta\}^T [K_e]\{\delta\} - (1/2)\{\delta\}^T \{P_e^{thermal}\} \quad (17)$$

where,

$[K_e] = \iint [B]^T [D][B] dxdy$ is the stiffness matrix,

$\{P_e^{thermal}\} = \iint [B]^T [f^{thermal}] dxdy$ is hygrothermally induced elemental load vector.

By minimizing the Equation (17) with respect to $\{\delta\}$, we get

$$[K_e]\{\delta\} = \{P_e^{hygrotherma}\} \quad (18)$$

For the thermal buckling analysis, in the first step, a static problem is solved as per governing equation (18) to calculate thermal stresses at the Gauss points of different elements for assumed temperature/moisture concentration rise or fall. Finally, these thermal stresses are used to form the matrix $[S^k]$ of the geometric stiffness matrix and the linear thermal buckling problem is solved as eigen value problem using Equation (19)

$$[K_e]\{\delta\} = \lambda[K_{ge}]\{\delta\} \quad (19)$$

where λ is buckling load factor.

The skyline storage technique is used to store global stiffness matrix in single array and simultaneous iteration technique is used for solving the buckling equation (19).

3. Results and Discussion

Convergence and Validation study: For convergence and validation study, 10-layered simply supported angle-ply laminated composite plate $(\theta^0/-\theta^0/\theta^0/-\theta^0 \ldots_{10})$is taken. Material properties are taken as: $E_1/E_2 = 15, G_{12} = G_{13} = 0.5E_2,\ G_{23} = 0.3356E_2, \nu_{12} = 0.3, \nu_{23} = 0.49, \alpha_1/\alpha_0 = 0.015, \alpha_2/\alpha_0 = 1, \alpha_2 = \alpha_3, \alpha_0 = 10^{-6}$. Plate is subjected to equal rise or fall of temperature at top and bottom surfaces. Sinusoidal temperature variation is taken as: $\Delta T(x, y, \pm h/2) = T_0 \sin(\pi x/a) \sin(\pi y/b)$. The results for non-dimensional buckling load $(\emptyset = \alpha_0 T_{cr})$ are reported in Table 1 $(T_0 = 1.0)$. It can be seen that the present results converge at mesh size of 12x12. Hence, in further studies same mesh size is taken. Present results are compared with the 3D elasticity-based results given by Noor and Burton [22], 2 different FEs (9 d.o.f and 11 d.o.f. per node) based higher-order shear deformation theory (HOSDT9,HOSDT11) by Babu and Kant [26] and Fourier series based global-local higher order theory (GLHOT) published by Matsunaga [27]. It is observed that the present model is able to predict resultsmore accurately when compared with the 3D elastic solutions even for thick plates. $(\%\ error = \frac{Present\ -3D\ elasticity}{3D\ elasticity} \times 100)$. It is seen that for thick plates, maximum % error is observed as 0.35%. with increase in thickness to side ratio (h/a) of the plate, non-dimensional buckling load increases. Fig. 3 shows fundamental buckling mode shape for h/a=0.01 and angle of ply equals 0°.

Table 2 shows results for non-dimensional buckling load for same plate with all sides clamped boundary condition. It is seen that, with increase in thickness ratio (h/a), non-dimensional critical buckling load increases as expected. Also, the clamped plate shows buckling at higher temperature as compared to simply supported plate. Thus, the present model is able to predict the non-dimensional buckling load especially for thick plates efficiently without using any post-processing technique. It is seen that the maximum value of non-dimensional buckling load is observed at 45°.

Table 1. Convergence and validation of non-dimensional critical buckling load (∅) for square shaped simply supported 10-layered angle-ply laminated composite plate subjected to equal rise or fall of temperature at top and bottom surfaces (values inside parenthesis indicates mesh size).

h/a	Source	θ^0		
		0°	15°	30°
0.01	Present (8x8)	0.7470^{-3}	0.1122^{-2}	0.1508^{-2}
	Present (12x12)	0.7465^{-3}	0.1117^{-2}	0.1502^{-2}
	Present (16x16)	0.7465^{-3}	0.1117^{-2}	0.1502^{-2}
	3D Elasticity [22]	0.7463^{-3}	0.1115^{-2}	0.1502^{-2}
	% Error	0.02	0.17	0.000
	HOSDT11 [26]	0.7471^{-3}	0.1116^{-2}	0.1502^{-2}
	HOSDT9 [26]	0.7470^{-3}	0.1116^{-2}	0.1502^{-2}
	GLHOT [27]	0.7463^{-3}	0.1115^{-2}	0.1502^{-2}
0.20	Present	0.1466^{-0}	0.1759^{-0}	0.2378^{-0}
	3D Elasticity [22]	0.1463^{-0}	0.1753^{-0}	0.2377^{-0}
	% Error	0.20	0.34	0.04
	HOSDT11 [26]	0.1441^{-0}	0.1773^{-0}	0.2449^{-0}
	HOSDT9 [26]	0.1417^{-0}	0.1764^{-0}	0.2421^{-0}
	GLHOT [27]	0.1436^{-0}	0.1765^{-0}	0.2432^{-0}

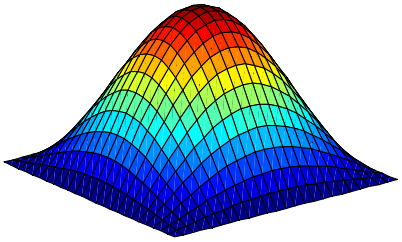

Fig. 3. Non-dimensional fundamental buckling mode shape for 10-layered angle-ply laminated composite plate (h/a=0.01).

Table 2. Non-dimensional critical buckling load (∅) for square shaped clamped 10-layered angle-ply laminated composite plate subjected to equal rise or fall of temperature at top and bottom surfaces.

h/a	θ^0			
	0°	15°	30°	45°
0.01	0.1891^{-2}	0.2317^{-2}	0.3413^{-2}	0.3447^{-2}
0.02	0.7275^{-2}	0.8880^{-2}	0.1306^{-1}	0.1323^{-1}
0.05	0.3729^{-1}	0.4450^{-1}	0.6630^{-1}	0.6892^{-1}
0.10	0.9758^{-1}	0.1116^{-0}	0.1581^{-0}	0.1810^{-0}
0.20	0.1870^{-0}	0.2068^{-0}	0.2702^{-0}	0.3191^{-0}

4. Conclusion

In the present work, a recently proposed third-order in-plane displacement field based zigzag theory was used for the buckling analysis of laminated composite plates under thermal conditions. for transverse displacement field, quadratic variation was taken for core layer while constant for face layers. Zigzag effects were incorporated using linear Heaviside unit step function. Proposed theory satisfies inter-laminar stress continuity condition at interface along with zero values at top and bottom surfaces. The proposed theory was free from any kind of penalty requirement or post-processing technique. Nine-noded C-0 finite element having twelve d.o.f. per node was used. The efficiency of the proposed model was studied by comparing the present results with those available in literature and were found to be in good agreement.

Disclosures

Free Access to this article is sponsored by SARL ALPHA CRISTO INDUSTRIAL.

References

1. Garg A, Chalak HD. Efficient 2D C0 FE based HOZT for analysis of singly curved laminated composite shell structures under point load. Journal of Physics: Conference Series, 2019; 1240(1):012014.
2. Fu Y, Li S, Y Jiang. Analysis of inter-laminar stresses for composite laminated plate with interfacial damage. Acta Mechanica Solida Sinica 2008; 21:127–40.

3. Chandrashekhara K. Thermal buckling of laminated plates using a shear flexible finite element. Finite Element in Analysis and Design 1992; 12:51–61.
4. Sai Ram KS, Sinha PK. Hygrothermal effects on the buckling of laminated composite plates. Composite Structures 1992; 21:233–247.
5. Pai PF. A new look at shear correction factors and warping functions of anisotropic laminates. International Journal of Solids and Structures 1995; 32(16):2295–2313.
6. Singh G, Rao GV, Iyengar NGR. Thermal postbuckling behavior of laminated composite plates. AIAA Journal 1994; 32:1336–1338.
7. Dafedar JB, Desai YM. Thermomechanical buckling of laminated composite plates using mixed, higher-order analytical formulation. Journal of Applied Mechanics 2002; 69:790-799.
8. Singh BN, Verma VK. Hygrothermal effects on the buckling of laminated composite plates with random geometric and material properties. Journal of Reinforced Plastics and Composites 2009; 28:409–427.
9. Kumar R, Singh D. Hygrothermal buckling response of laminated composite plates with random material properties: micro-mechanical model. Applied Mechanics and Materials 2011; 110–116:113–119.
10. Emam S, Eltaher MA. Buckling and postbuckling of composite beams in hygrothermal environments. Composite Structures 2016; 152:665–675.
11. Shu X, Sun L. Thermomechanical buckling of laminated composite plates with higher-order transverse shear deformation. Computers and Structures 1994; 53:1–7.
12. Chakrabarti A, Chalak HD, Iqbal MA, Sheikh AH. A new FE model based on higher order zigzag theory for the analysis of laminated sandwich beam with soft core. Composite Structures 2011; 93:271-279.
13. Lee J. Thermally induced buckling of laminated composites by a layerwise theory. Computers and Structures 1997; 65:917–922.
14. Shariyat M. Thermal buckling analysis of rectangular composite plates with temperature-dependent properties based on a layerwise theory, Thin-Walled Structures 2007; 45:439–452.
15. Chalak HD, Chakrabarti A, Sheikh AH, Iqbal MA. C0 FE model based on HOZT for the analysis of laminated soft core skew sandwich plates: Bending and vibration. Applied Mathematical Modelling 2014; 38:1211-1223.
16. Kapuria S, Dumir PC, Ahmed A. An efficient higher order zigzag theory for composite and sandwich beams subjected to thermal loading. International Journal of Solids and Structures 2003; 40:6613–6631.
17. Kapuria S, Achary GGS. An efficient higher order zigzag theory for laminated plates subjected to thermal loading. International Journal of Solids and Structures 2004; 41:4661–4684.
18. Khandelwal RP, Chakrabarti A, Bhargava P. Efficient 2D thermo-mechanical analysis of composites and sandwich laminates. Mechanics of Advanced Materials and Structures 2019; 26(6):526-538.
19. Garg N, Karkhanis RS, Sahoo R, Maiti PK, Singh BN. Trigonometric zigzag theory for static analysis of laminated composite and sandwich plates under hygrothermo-mechanical loading. Composite Structures 2019; 209:460–471.
20. Garg A, Chalak HD. Analysis of non-skew and skew laminated composite and sandwich plates under hygro-thermomechanical conditions including transverse stress variations. Journal of Sandwich Structures and Materials 2020; 0(0):1-24.
21. Noor AK, Burton WS. Three-dimensional solutions for thermal buckling of multi-layered anisotropic plates. ASCE Journal of Engineering Mechanics 1992; 118(4):683–701.
22. Noor AK, Burton WS. Three-dimensional solutions for the free vibration and buckling of thermally stressed multi-layered angle-ply composite plates. ASME Journal of Applied Mechanics 1992; 59(4):868–877.
23. Garg A, Chalak HD. A review on analysis of laminated composite and sandwich structures under hygrothermal conditions. Thin-Walled Structures 2019; 142:205-226.
24. Chalak HD, Chakrabarti A, Sheikh AH, Iqbal MA. Stability analysis of laminated soft core sandwich plates using higher order zig-zag plate theory. Mechanics of Advanced Materials and Structures 2015; 22(11):897-907.
25. Garg A, Chalak HD. Free vibration analysis of laminated sandwich plates under thermal loading. IOP Conference Series: Materials Science and Engineering 2020; 872(1):012055.
26. Babu CS, Kant T. Refined higher order finite element models for thermal buckling of laminated composite and sandwich plates. Journal of Thermal Stresses 2000; 23:111–130.
27. Matsunaga H. Thermal buckling of angle-ply laminated composite and sandwich plates according to a global higher-order deformation theory. Composite Structures 2006; 72:177–192.